Supplementary material (ESI) for Journal of Materials Chemistry

Supporting Information

Syntheses, structures, and magnetic properties of heterometallic coordination polymers with carboxyphosphonate linkers

Zhi-Guo Gu, Slaci C. Sevov

Department of Chemistry and Biochemistry,
University of Notre Dame, Notre Dame, Indiana 46556

ssevov@nd.edu

Table S1 Selected bond lengths (Å) for **1-CuMn**, **2-CuCo**, **3-CuCd**, **4-CuLa** and **5-CuNd**

		1-CuMn			
Mn(1)–O(13A)	2.049(2)	Mn(1)–O(17)	2.133(2)	Mn(1)–O(7)	2.160(2)
Mn(1)–O(15)	2.175(3)	Mn(1)–O(11B)	2.199(2)	Mn(1)–O(16)	2.243(3)
Mn(2)–O(6)	2.098(2)	Mn(2)–O(12)	2.121(2)	Mn(2)–O(21)	2.188(2)
Mn(2)–O(18)	2.213(2)	Mn(2)–O(20)	2.235(2)	Mn(2)–O(19)	2.270(3)
Cu(1)–O(14A)	1.894(2)	Cu(1)–O(3)	1.965(2)	Cu(1)–O(1)	1.978(2)
Cu(1)–N(1)	2.021(2)	Cu(1)–O(7)	2.281(2)	Cu(2)–O(5)	1.914(2)
Cu(2)–O(8)	1.940(3)	Cu(2)–O(10)	1.960(2)	Cu(2)–N(2)	2.015(3)
Cu(2)–O(12)	2.317(2)	Symmetry codes: A $x + 1/2, -y + 1/2, z - 1/2$; B $x + 1, y, z$			
		2-CuCo			
Co(1)–O(13A)	1.967(3)	Co(1)–O(17)	2.012(3)	Co(1)–O(7)	2.128(2)
Co(1)–O(15)	2.078(3)	Co(1)–O(11B)	2.121(3)	Co(1)–O(16)	2.202(4)
Co(2)–O(6)	2.054(2)	Co(2)–O(12)	2.065(2)	Co(2)–O(21)	2.086(3)
Co(2)–O(18)	2.118(3)	Co(2)–O(20)	2.147(3)	Co(2)–O(19)	2.146(3)
Cu(1)–O(14A)	1.889(3)	Cu(1)–O(3)	1.963(3)	Cu(1)–O(1)	1.974(3)
Cu(1)–N(1)	2.015(3)	Cu(1)–O(7)	2.259(2)	Cu(2)–O(5)	1.909(2)
Cu(2)–O(8)	1.947(3)	Cu(2)–O(10)	1.957(3)	Cu(2)–N(2)	2.008(3)
Cu(2)–O(12)	2.297(2)	Symmetry codes: A $x + 1/2, -y + 1/2, z - 1/2$; B $x + 1, y, z$			
		3-CuCd			
Cd(1)–O(13A)	2.105(4)	Cd(1)–O(17)	2.164(4)	Cd(1)–O(7)	2.242(3)
Cd(1)–O(15)	2.252(5)	Cd(1)–O(11B)	2.272(4)	Cd(1)–O(16)	2.332(5)
Cd(2)–O(6)	2.208(3)	Cd(2)–O(12)	2.212(4)	Cd(2)–O(21)	2.277(4)
Cd(2)–O(18)	2.307(4)	Cd(2)–O(20)	2.318(4)	Cd(2)–O(19)	2.349(4)
Cu(1)–O(14A)	1.899(4)	Cu(1)–O(3)	1.971(4)	Cu(1)–O(1)	1.988(4)
Cu(1)–N(1)	2.021(4)	Cu(1)–O(7)	2.240(3)	Cu(2)–O(5)	1.917(4)
Cu(2)–O(8)	1.934(4)	Cu(2)–O(10)	1.956(4)	Cu(2)–N(2)	2.022(4)
Cu(2)–O(12)	2.286(4)	Symmetry codes: A $x + 1/2, -y + 1/2, z - 1/2$; B $x + 1, y, z$			
		4-CuLa			
Cu(1)–O(6)	1.934(3)	Cu(1)–O(1A)	1.953(3)	Cu(1)–O(3A)	1.962(3)
Cu(1)–N(1A)	2.019(3)	Cu(1)–O(13)	2.637(3)	Cu(1)–O(7A)	2.530(3)
La(1)–O(5)	2.466(3)	La(1)–O(11)	2.532(3)	La(1)–O(2B)	2.540(3)
La(1)–O(9)	2.557(3)	La(1)–O(10)	2.562(3)	La(1)–O(8)	2.632(3)
La(1)–O(3C)	2.639(3)	La(1)–O(4C)	2.765(3)	La(1)–O(7A)	2.450(3)
Symmetry codes: A $x, -y + 1/2, z + 1/2$; B $x - 1, y, z$; C $x, y, z + 1$					
		5-CuNd			
Cu(1)–O(6)	1.927(2)	Cu(1)–O(1A)	1.952(2)	Cu(1)–O(3A)	1.962(2)
Cu(1)–N(1A)	2.004(3)	Cu(1)–O(13)	2.613(3)	Cu1(1)–O(7A)	2.591(4)
Nd(1)–O(5)	2.420(2)	Nd(1)–O(11)	2.477(2)	Nd(1)–O(2B)	2.483(2)
Nd(1)–O(9)	2.508(2)	Nd(1)–O(10)	2.506(2)	Nd(1)–O(8)	2.566(2)
Nd(1)–O(3C)	2.577(2)	Nd(1)–O(4C)	2.735(2)	Nd(1)–O(7A)	2.384(2)
Symmetry codes: A $x, -y + 1/2, z + 1/2$; B $x - 1, y, z$; C $x, y, z + 1$					

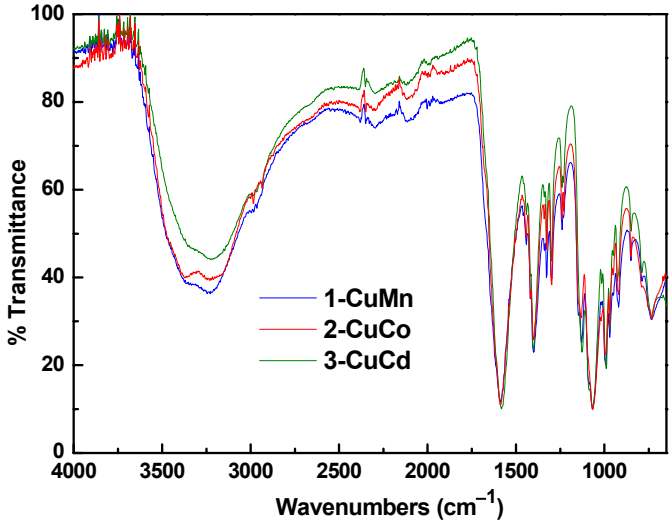

Fig. S1 FT-IR spectroscopy for as-synthesized samples of **1-CuMn**, **2-CuCo** and **3-CuCd**.

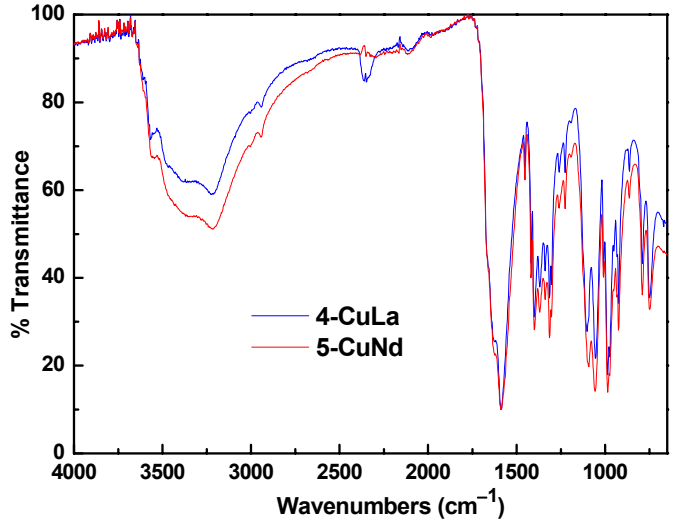

Fig. S2 FT-IR spectroscopy for as-synthesized samples of **4-CuLa** and **5-CuNd**.

FT-IR (cm^{-1}) data for: **1-CuMn**: 3335 (br), 2923 (w), 1588 (s), 1443 (w), 1400 (s), 1327 (m), 1297 (m), 1239 (w), 1132 (m), 1068 (s), 992 (m), 966 (w), 921 (m), 850 (w), 788 (w), 735 (m); **2-CuCo**: 3372 (br), 2931 (w), 1586 (s), 1446 (w), 1402 (s), 1326 (m), 1298 (m), 1241 (w), 1135 (m), 1066 (s), 996 (m), 971 (w), 921 (m), 850 (w), 791 (w), 733 (m); **3-CuCd**: 3373 (br), 2935 (w), 1587 (s), 1443 (w), 1402 (s), 1326 (m), 1298 (m), 1242 (w), 1135 (m), 1066 (s), 996 (m), 971 (w), 921 (m), 850 (w), 789 (w), 733 (m); **4-CuLa**: 3362 (br), 2942 (w), 1588 (s), 1450 (w), 1400 (s), 1368 (m), 1339 (m), 1314 (m), 1303 (m), 1259 (w), 1227 (w), 1102 (m), 1055 (m), 986 (m), 973 (w), 925 (m), 863 (w), 791 (m), 749 (m); **5-CuNd**: 3347 (br), 2942 (w), 1589 (s), 1452 (w), 1400 (s), 1369 (m), 1339 (m), 1314 (m), 1303 (m), 1259 (w), 1227 (w), 1093 (m), 1057 (m), 986 (m), 973 (w), 925 (m), 863 (w), 791 (m), 750 (m).

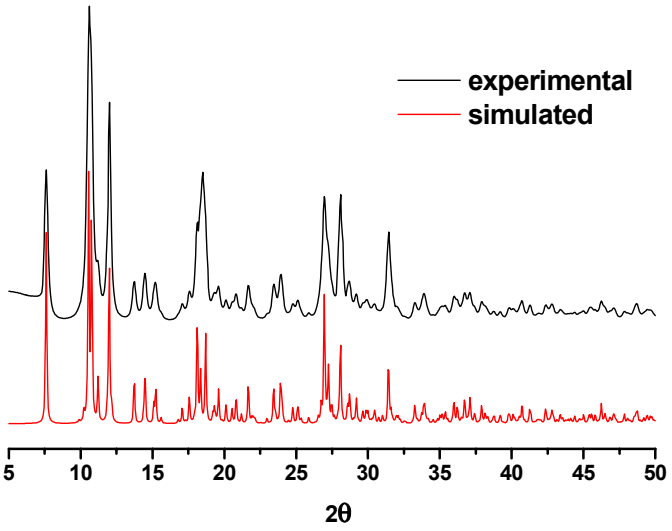

Fig. S3 PXRD patterns of **1-CuMn** as-synthesized sample and simulated one based on the single-crystal structures.

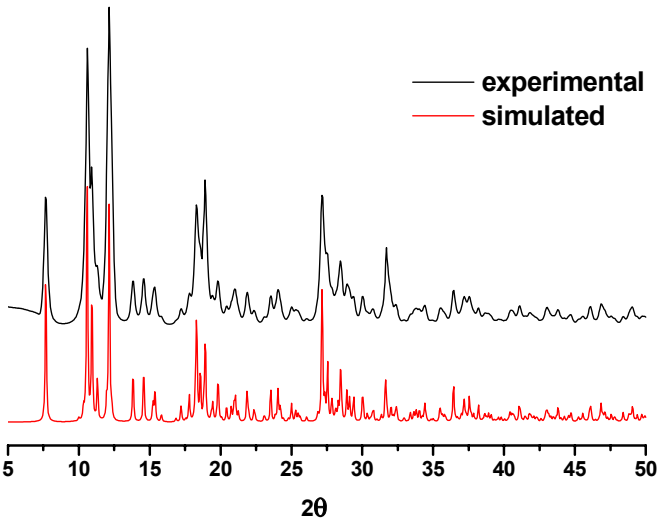

Fig. S4 PXRD patterns of **2-CuCo** as-synthesized sample and simulated one based on the single-crystal structures.

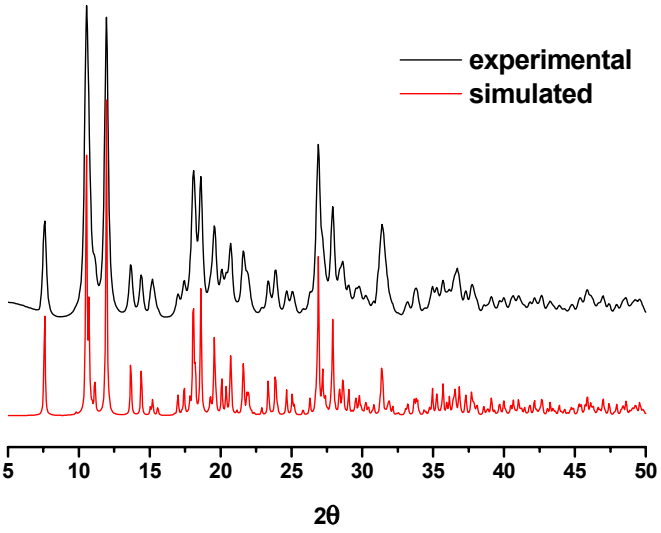

Fig. S5 PXRD patterns of **3-CuCd** as-synthesized sample and simulated one based on the single-crystal structures.

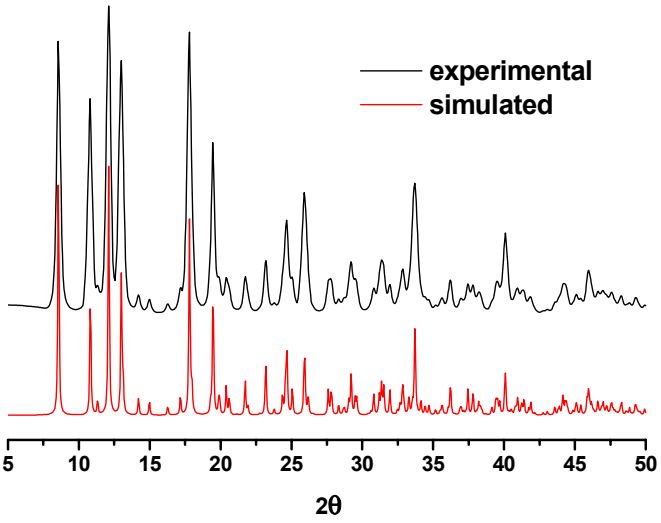

Fig. S6 PXRD patterns of **4-CuLa** as-synthesized sample and simulated one based on the single-crystal structures.

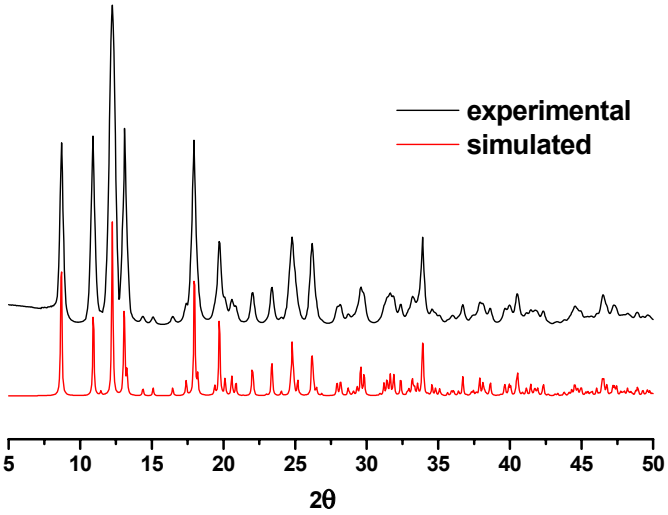

Fig. S7. PXRD patterns of **5-CuNd** as-synthesized sample and simulated one based on the single-crystal structures.

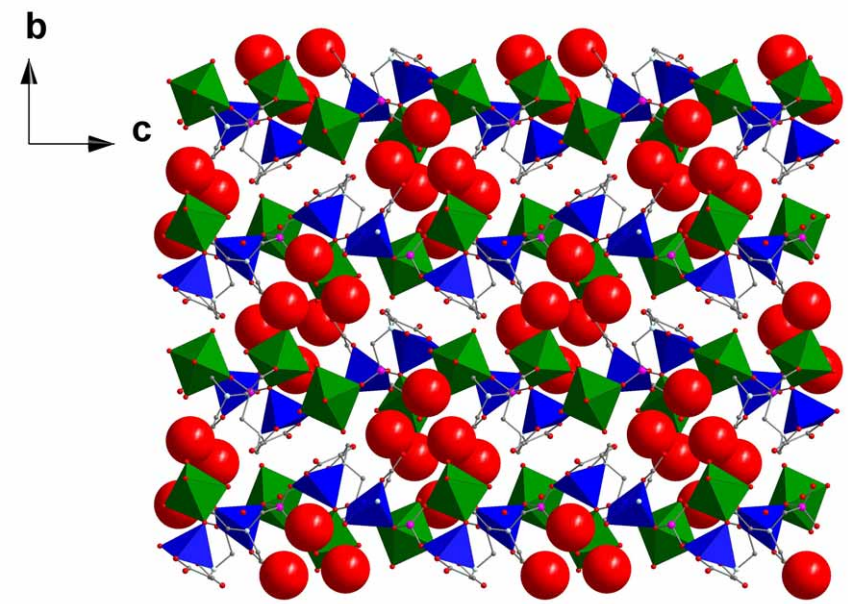

Fig. S8 Polyhedral representation of the structure in **1-CuMn** along the *a*-axis showing the layers parallel to the *bc* plane being interconnected by hydrogen bonds between uncoordinated water molecules. Color code: Cu, blue; Mn, green; P, purple; O, red; N, sky blue; C, gray.

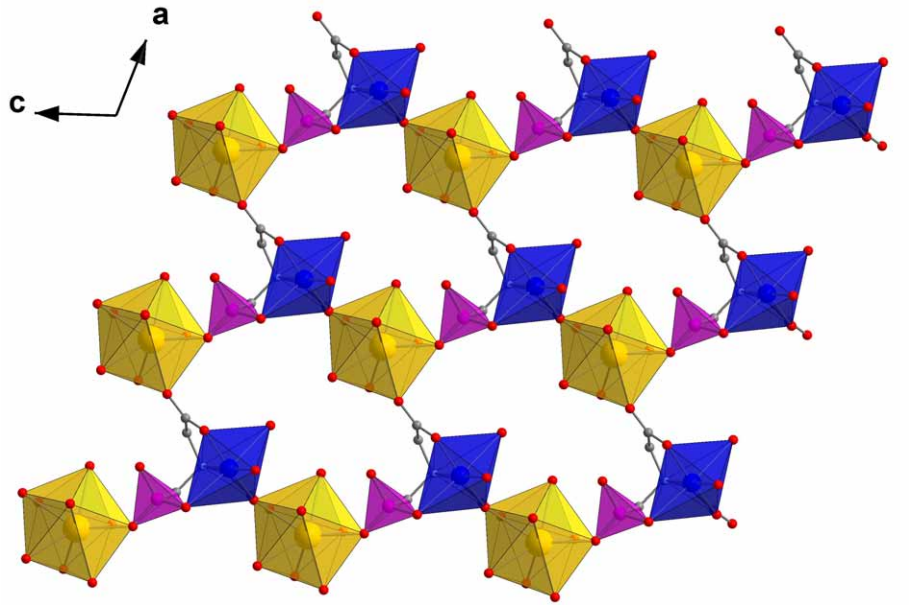

Fig. S9 Polyhedral representation of the single layer in **4-CuLa** along the *b*-axis. Color code: Cu, blue; La, yellow; P, purple; O, red; N, sky blue; C, gray.

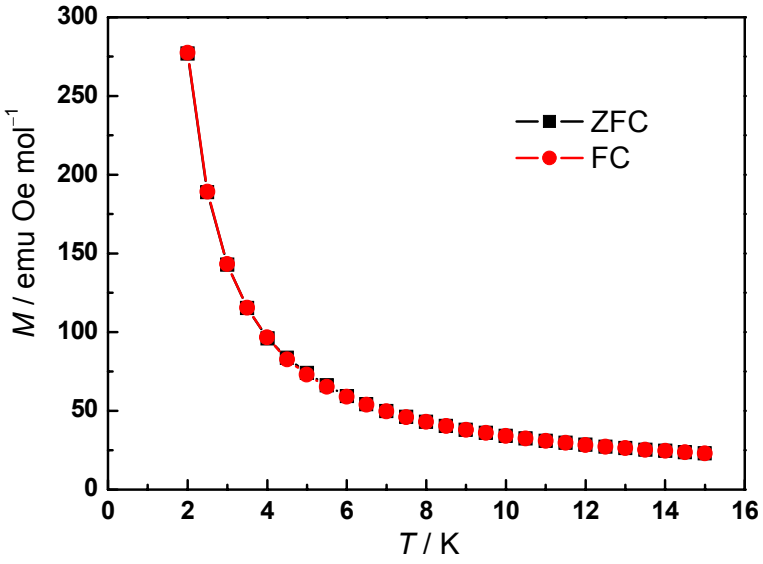

Fig. S10 Zero field cooled magnetization (ZFCM) and field cooled magnetization (FCM) versus T measures at 50 Oe for **1-CuMn**.